Korean J. Chem. Eng., 36(2), 217-225 (2019)
DOI: 10.1007/s11814-018-0166-x

pISSN: 0256-1115
eISSN: 1975-7220

Degradation and removal of *p*-nitroaniline from aqueous solutions using a novel semi-fluid Fe/charcoal micro-electrolysis reactor

Mohammad Malakootian*,, Mostafa Pournamdari***, Ali Asadipour****, and Hakimeh Mahdizadeh**,†**

*Environmental Health Engineering Research Center, Kerman University of Medical Sciences, Kerman, Iran
**Department of Environmental Health, School of Public Health, Kerman University of Medical Sciences, Kerman, Iran
***Department of Food and Drug Control, Faculty of Pharmacy, Kerman University of Medical Sciences, Kerman, Iran
****Department of Medicinal Chemistry, Faculty of Pharmacy, Kerman University of Medical Sciences, Kerman, Iran
(*Received 17 June 2018 • accepted 10 October 2018*)

Abstract−*p*-Nitroaniline (PNA) is a common contaminant in the wastewater of oil refineries, the petrochemical industry and from production of pesticides, dyes and glue. The aim of this research was to determine the extent of degradation and removal of PNA from aqueous solutions by a novel semi-fluid Fe/charcoal reactor, process optimization, determination of the intermediate and final products and the degradation reaction path. The effective factors in the degradation process were contact time, aeration amount, initial PNA concentration, Fe/charcoal ratio, and initial pH of the solution. The intermediate products were determined by GC-MS. The kinetics of the degradation reaction also was determined. PNA removal efficiency in an actual sample from petrochemical industry wastewater was tested under optimal conditions. The maximum removal efficiency under the optimal conditions (pH: 7; contact time 120 min; aeration rate 10 L/min; Fe/charcoal ratio: 2/1; initial concentration of PNA: 10 mg/L) for the synthetic solution and in actual wastewater samples were 95% and 89%, respectively. In addition, the system stability was investigated in ten consecutive cycles of the electrode reuse. The removal efficiency decreased as low as 5%, which indicates the high stability of the system. The degradation process was determined to follow *pseudo*-first kinetics and the Langmuir-Hinshelwood model. Fe/charcoal micro-electrolysis is a relatively highly efficient system for removing PNA from wastewater and is suggested for this purpose.

Keywords: Micro-electrolysis, Fe/Charcoal, PNA, Galvanic Cells, Degradation

INTRODUCTION

Increases in contamination by industrial wastewater have caused rapid degradation of ecological systems and clean water resources. *p*-Nitroaniline (PNA), an aniline derivative, is a common contaminant in the wastewater of many industries, including oil refineries, the petrochemical industry and producers of pesticides, dyes and glue [1,2]. This compound is an important precursor in the synthesis of organic compounds, azo dyes, disinfectants, and medicine, and is used to purify and synthesize drugs. According to the United States Environmental Protection Agency (UEPA), this material is the top contaminant in water because of its toxicity, carcinogenicity, and mutagenicity. The threshold limit value (TLV) of PNA is 0.001 kg/m^3. Even at trace concentrations, it is very hazardous for aquatic life and human health and causes serious environmental problems [1-5].

One of the technologies employed in wastewater treatment is the advanced oxidation process (AOP), which produces hydroxyl radicals ($OH^•$); they are the important oxidants in the degradation of organic compounds. The final products produced by AOP include H_2O, CO_2, and other mineral ions, which pose no threat to the environment [6-10]. Although AOP shows a high degradation capacity, it has limitations such as low COD removal, low stability, and the high cost of wastewater treatment in industrial uses of this process. Thus, research has been directed to the development of new water and wastewater treatment methods for degrading organic compounds and toxic materials from factories [11-13].

Iron-carbon (Fe/C) micro-electrolysis is a developed AOP technology that is low cost and highly efficient for treating wastewater from the pharmaceutical, oil, chemical and petrochemical industries [14,15]. In this system, small iron and carbon pieces are typically used as electrodes through which a large number of microscopic galvanic cells are formed [15]. In Fe-C micro-electrolysis systems, Fe^0 acts as the anode, which loses two electrons and produces Fe^{2+}. The current conductivity of the cathode intensifies the reduction by receiving electrons and transferring them to the contaminants or oxygen under aerobic conditions [14,16]. A potential difference develops between the small iron pieces and carbon, both of which are porous materials. The cellular reactions of the Fe-C micro-electrolysis system are shown in Eqs. (1)-(4) [14,15,17,18].

Anode: $Fe-2e \rightarrow Fe^{2+}$ E^0 (Fe^{2+}/Fe)=−0.44 V (1)

Cathode: under acidic conditions:
$2H^+ + 2e \rightarrow 2[H] \rightarrow H_2$ E^0 (H^+/H_2)=0.00 V (2)

Acidic conditions with oxygen:
$O_2 + 4H^+ + 4e \rightarrow 2O^• + 4[H] \rightarrow 2H_2$ E^0 (O_2/H_2O)=+1.23 V (3)

Neutral to alkaline conditions:
$O_2 + H_2O + 4e \rightarrow 4\,OH^-$ E^0 (O_2/OH^-)=+0.40 V (4)

†To whom correspondence should be addressed.
E-mail: H.Mahdizadeh2018@gmail.com

The [H] and O• oxidants and radicals produced from electrode reactions have high chemical activity such that they can degrade the carbon chains of organic compounds and fully convert them into CO_2, H_2O and other mineral compounds. Further, ferric ions (Fe^{3+}) are formed under the aerobic conditions through oxidation of ferro iron (Fe^{2+}), which leads to the formation of ferrous hydroxide [$Fe(OH)_2$] and ferric hydroxide [$Fe(OH)_3$], which are suitable flocculants for removing organic contaminants [14,17].

Zhou et al. used active granulated Fe-C micro-electrolysis systems to detect the degradation products of ionic liquids [19]. Lai et al. used them for degradation of 2, 3-iminobis-propanenitrile [20]. Deng et al. employed them to absorb phosphorus from aqueous solutions [21] and Lin et al. used these systems to treat wastewater-containing dinitrodiazophenol [11].

Studies using fixed-bed micro-electrolysis systems have experienced problems, including deactivation and blockage of the electrode materials [14]. In these micro-electrolysis systems, active granulated carbon was used as the cathode electrode. To improve their performance, achieve a higher extent of degradation, and overcome the problems of existing micro-electrolysis systems, a semi-fluid reactor was designed.

During adsorption, mineralization of organic compounds does not occur and the contaminants lose their liquid phase and enter a solid phase for which the problem of the presence of the contaminant still exists [22]. To minimize the effect of interference in the adsorption process in the oxidation reaction, the present study used cretacolor compressed charcoal instead of active granulated carbon. Furthermore, the extent of adsorption of PNA onto the charcoal and scrap iron was investigated. The aim of this research was to investigate the extent of degradation and removal of PNA from aqueous solutions by a Fe/charcoal semi-fluidized micro-electrolysis reactor. Process optimization and determination of the intermediate and final products and the degradation reaction path were carried out to this end. This system has a high potential for degradation of many organic and toxic contaminants and can be used extensively to decontaminate water and wastewater.

MATERIALS AND METHODS

This experimental study was conducted in the Environmental Health Engineering Research Center of Kerman University of Medical Sciences.

1. Materials

Iron chips were obtained from iron waste that had been discarded by metalsmithing workshops. The chips, which were used as the anode electrode, were separated from the surrounding trash using a magnet and were screened (iron size was 3 to 6 mm). Cretacolor compressed charcoal with a size of 3-6 mm was used as the cathode electrode. Initially, the iron chips were washed with a diluted hydroxide solution for several seconds to remove fats. Then, they were put in a diluted solution of HNO_3 for several seconds to activate the surface oxidation of iron; eventually, the electrode material was washed with distilled water several times before use in the reactor. PNA with a purity of 99.8% and ethyl acetate were purchased from Merck (Germany). The ethyl acetate solvent underwent distillation twice before use in GC-MS analysis. All of the synthetic solutions were prepared using double-distilled water.

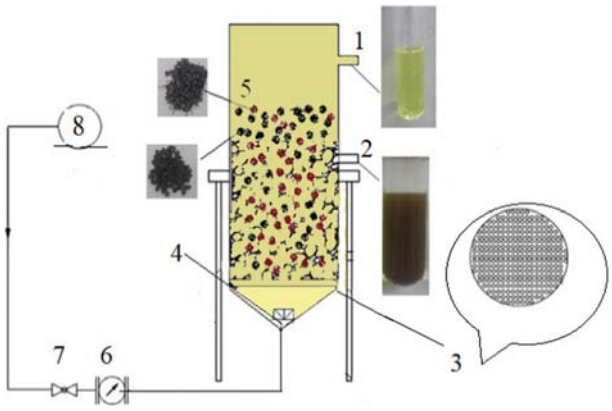

Fig. 1. Fe/charcoal micro-electrolysis reactor.

1. Solution input	5. Float electrode material
2. Sampling point	6. Flowmeter
3. Lattice plate	7. Valve
4. Air bubble	8. Air pump

2. Fabrication and Operation of the Reactor

An air pump, rubber pipes, air bubble disperser and a Plexiglas cylinder with an approximate volume of 350 ml were used to create the Fe/charcoal micro-electrolysis reactor. The reactor was then filled with a specific volume of the electrode material (iron chips and charcoal). A schematic of the reactor is shown in Fig. 1.

First, the synthetic PNA solutions were prepared to the specified concentrations. Thereafter, 250 ml of the solution of interest was used. The pH of the solution was adjusted by sulfuric, acid and sodium hydroxide 0.1 N solution as needed and then poured into the reactor. The reactor contents were kept half-floating by the air pump. After the reaction for a specified duration, a specific volume of the solution was taken from the reactor and filtered through a polytetrafluoroethylene (PTFE) 0.45 μm syringe filter. The initial and final concentrations of PNA in the synthetic solutions were measured with an ultraviolet spectrophotometer (Shimadzu 1800) at a wavelength of 381 nm. All of the experiments were performed at room temperature.

The effect of the variables of pH (3, 5, 7, 9 and 11), initial concentration of PNA (10, 15, 20 and 25 ppm), air flow rate (0, 5, 10 and 20 L/min), Fe/charcoal ratio (0/1, 1/0, 2/1, 1/1 and 1/2) and contact time (10, 15, 30, 45, 60, 75, 90, 105, 115 and 120 min) on the extent of degradation and removal of PNA was evaluated and the optimal level of each variable was determined. To enhance the confidence coefficient and accuracy, the experiments were replicated three times. Gas chromatography-mass spectrometry (GC-MS; 7890A/7693 series, Agilent; USA) was used to investigate the extent of PNA degradation in the real wastewater sample from the petrochemical industry (under optimal conditions).

3. Characterization

After the reaction, some of the effluent of the reactor (without electrode materials) was withdrawn. This effluent was turbid and contained colloidal and suspended solids, which became stationary after 60 min, during which the flocs resulting from the electrochemical processes precipitated. The flocs precipitated as a solid or sludge and were then dried in an oven at 70 °C for 24 h. To deter-

mine the chemical characteristics of the sludge, Fourier transform infrared spectroscopy (FTIR; 6300 Japan) was employed.

4. GC-MS Analyze

GC-MS was used to determine the degradation reaction pathways of the PNA and its intermediate and final byproducts. The characteristics of the GC-MS are as follows: Agilent HP-5MS column (L: 30 m; ID: 250 μm; FT: 0.25 μm), He carrier gas (flow 0.8 mL/min), 1 μL splitless injection at 250 °C; initial oven temperature of 40 °C held for 3 min and then increased to 250 °C (at 5 °C/min) with a final hold for 10 min. The ion source and quadrupole of the MS were set at 230 and 150 °C, respectively, and the mass range was 35 to 540 amu. GC-MS was carried out in the total ion chromatogram (TIC) and extracted ion chromatogram (EIC) modes. MSD chemstation software and the NIST (library version 08), respectively, were used to monitor the instrument and establish the structure of the byproducts [23,24].

4-1. Preparation of Samples

Synthetic PNA solution (10 ppm, 250 mL) and real wastewater sample were treated with Fe/charcoal micro-electrolysis reactor under optimum conditions. Aliquots of 1 mL of the effluent were taken at intevals of 0, 5, 10, 15, 30, 60, 75, 120, and 180 min and kept at −20 °C until analysis was performed by GC-MS. A volume of 1 mL ethylacetate was added to each thawed sample; then, the mixtrue was vortexed and centrifuged at 4,000 rpm for 5 min. 300 μL of supernatant was then dried under jentle stream of N_2 and reconstituted with 150 μL of the solvent and finally analyzed by GC-MS method. To determine the intermediate products, the blank reactor, as control, was also assembled, while 250 mL demineralized PNA-free water was added into the reactor instead of the sample [24].

5. Investigation of Secondary Pollution of Iron Ions

A Shimadzu 670 (Japan) flame atomic absorption spectrometer was used to determine the secondary pollution of iron ions in the effluent of reactor discharge. The wavelength was set at 248.3 nm for Fe determination. 20 mL of the reactor effluent was kept in a stationary state for 2 hours to deposit chemical sludge resulted from electrochemical reactions. The supernatant was then filtered and analyzed using the instrument.

6. Stability of the System

In this study, the experiments were done in a batch system; thus stability of the system was investigated in ten consecutive cycles. Each cycle was performed under optimum conditions (Fe/charcoal: 2/1; pH: 7; time: 120 min; PNA: 10 mg/L; O_2: 10 L/min). After the end of each cycle, the electrode material was washed with distilled water and re-used in the reactor; the PNA removal efficiency was then investigated in each cycle.

Experiments and sampling were performed based on the techniques set forth in the Standard Method book (20th Ed.) [25]; the kinetics of the degradation reaction then were determined. Data analysis was performed using SPSS-16 software.

RESULTS AND DISCUSSION

1. Effect of Fe/Charcoal Ratio on PNA Removal Efficiency

When iron chips and charcoal are mixed and half-floated in the reactor, microscopic galvanic cells are formed among them. The number of cells is affected by the amount of contact between the iron chips and charcoal [14]. 60 g/L of iron and charcoal was studied at mass ratios (Fe/charcoal) of 2/1, 1/2, 1/1, 1/0 and 0/1 for its effect on PNA degradation efficiency. The results are compared in Fig. 2.

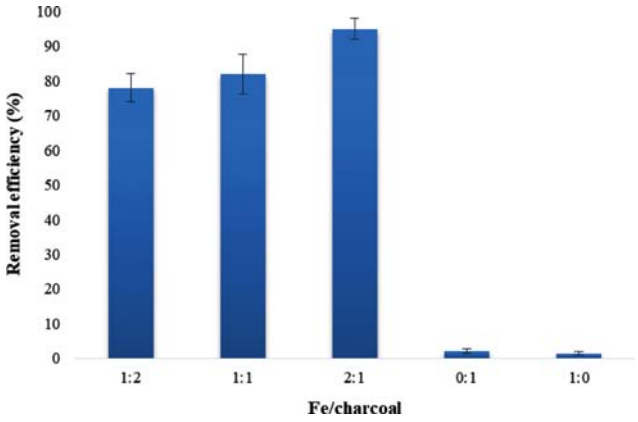

Fig. 2. Effect of Fe/charcoal on PNA removal efficiency under optimal conditions (pH: 7; time: 120 min; PNA: 10 mg/L; O_2: 10 L/min).

The extent of PNA degradation increased from 78% to 95% with an increase in the Fe/charcoal ratio from 1/2 to 2/1. In Fe/charcoal micro-electrolysis systems, iron particles liberate electrodes as the anode metal, while charcoal acts as the cathode and microscopic galvanic cells form between them. An increase in iron particles increases the number of microscopic galvanic cells and the radical production reactions in the micro-electrolysis system. These radicals increase the rate of PNA degradation. Furthermore, with an increase in the Fe/charcoal ratio, the number of Fe^{2+} ions and, in turn, ferro hydroxide, and ferric hydroxide ions increase, increasing precipitation [15,20].

In the study by Liu et al. for pretreatment of Lead 2, 4, 6-trinitroresorcinol wastewater by Fe-C internal electrolysis process, the COD removal efficiency increased with increasing iron amount, whereas it decreased in Fe-C ratio greater than 1/2. Liu et al. explained that these changes were due to the production of more micro primary cells, [H], Fe^{2+} and Fe^{3+} following the increase in iron amount. For Fe-C volume ratio greater than 1/2, the excess iron filings could cause an imbalance between iron and carbon electrodes, which reduced COD removal efficiency [16]. These findings are consistent with the results of the current study.

To investigate the extent of PNA adsorption by the iron electrode and charcoal in the Fe/charcoal micro-electrolysis system, two control experiments were performed: (1) application of the system with charcoal alone (Fe/charcoal=0/1); (2) application of the system with iron alone (Fe/charcoal=1/0). The maximum PNA adsorption by charcoal in the first and second systems was 2.5% and 1.6%, respectively (Fig. 2) which is negligible. It can be concluded that the adsorption process did not interfere with the electrochemical reactions of the Fe/charcoal micro-electrolysis system.

Yang et al. degraded sunset yellow (SY) dye using a Fe-C micro-electrolysis system; the total dosage of cast-iron scrap and granular activated carbon was fixed at 500 g/L; to reduce or remove the

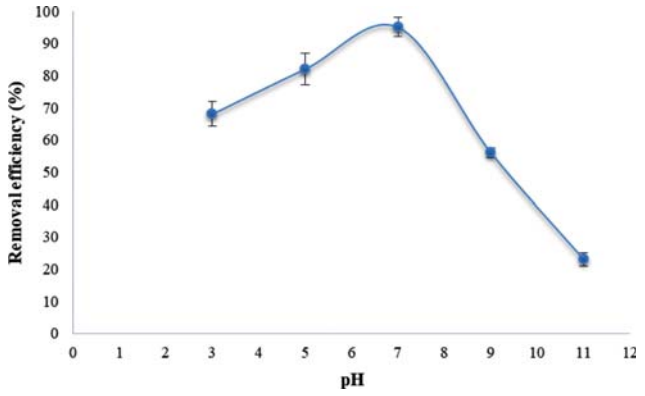

Fig. 3. Effect of initial pH of solution on PNA removal efficiency under optimal conditions (Fe/charcoal: 2/1; time: 120 min; PNA: 10 mg/L; O_2: 10 L/min).

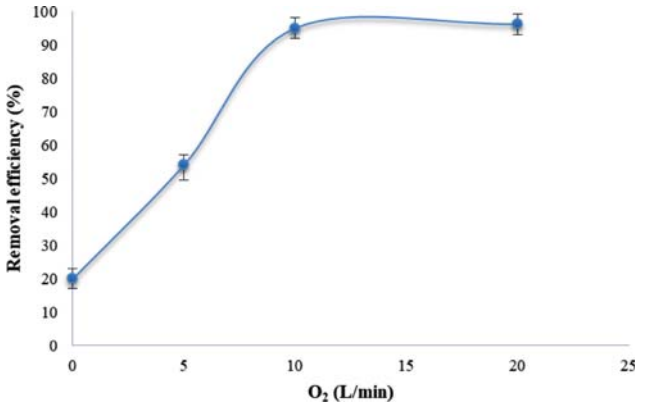

Fig. 4. Effect of O_2 on PNA removal efficiency under optimal conditions (Fe/charcoal: 2/1; time: 120 min; PNA: 10 mg/L; pH: 7).

effect of adsorption, the activated carbon was immersed in a dye-containing solution for 36 h until the carbon surface was saturated [14]. In the present study, by replacing the active carbon with compressed charcoal, the interference of the adsorption process in the electrochemical reaction was controlled. Furthermore, due to the high potential of the system to produce degrading radicals, fewer electrodes were consumed (almost eight-times less).

2. Effect of pH on PNA Removal Efficiency

The effect of the initial pH of the solution on PNA removal efficiency is shown in Fig. 3.

The redox potential and amount of [H] and O• radicals produced during micro-electrolysis are heavily affected by the initial pH of the solution. Furthermore, the pH of the solution alters the chemical status of the reactor contents. As shown in Eqs. (2) and (3), under acidic conditions, a high concentration of hydrogen ions [H^+] results in increased production of [H] and O• radicals [15]; however, the precipitation of the ferro and produced ferric ions becomes more difficult. The hydrogen produced under acidic conditions deactivates the iron and the Fe^{2+} interferes with PNA detection due to a reduction and color-rendering properties [14,15]. Under aerobic conditions, ferro ions convert to ferric ions, increasing the alkalinity of the solution. Iron hydroxides such as $Fe(OH)^{2+}$, $Fe(OH)_6^{3+}$ and $Fe(OH)_2$ form and cause precipitation of the sludge flocs. The intermediate products of the reaction are trapped in the flocs, precipitate during enmeshment, and are removed from the solution [14].

At high pH (alkaline conditions), the efficiency of Fe^{2+} ions declined significantly, thereby reducing PNA removal efficiency. The greatest extent of removal and precipitation of intermediate compounds occurred at neutral pH.

The study by Sun et al. for the decomposition of PNA with a solar photo-Fenton advanced oxidation process showed that the degradation efficiency of PNA was decreased from 99.92 to 3.83% within 60 min reaction when the pH of the solutions was increased from 3.0 to 6.0 [26]. They explained that the ferrous ion catalyst was deactivated and the oxidation potential of OH decreased in conditions of pH>4.0, resulting in a drastic decrease in removal efficiency of PNA [26]. Since pH of most water and wastewater flows range from 6 to 9, lower and higher pH values than this range would increase the cost of the process.

Yang et al. degraded SY dye using a Fe-C micro-electrolysis system in which the greatest dye removal efficiency was achieved under acidic conditions [14]. However, the iron hydroxides quickly precipitated in neutral environments and the intermediate products of the process were removed quickly. In addition, to reduce the costs associated with wastewater pH adjustment, neutral environment was chosen as optimal [14].

3. Effect of Aeration on PNA Removal Efficiency

As shown in Eqs. (5)-(7), aeration plays an important role in micro-electrolysis systems [6,14,15,27].

$$Fe - 2e \rightarrow Fe^{2+} \quad (5)$$

$$Fe^{2+} - e \rightarrow Fe^{3+} \quad (6)$$

$$O_2 + 2H^+ + 2e \rightarrow H_2O_2 \quad (7)$$

The results of aeration on PNA removal efficiency are shown in Fig. 4.

In this study, an increase in the aeration level from 0 to 10 L/min increased the removal efficiency from 20% to 95%. With the further increase in aeration to 20 L/min, the removal efficiency reached 96.2%; however, as further aeration was not economical, 10 L/min was chosen as the optimal aeration rate.

Aeration in micro-electrolysis systems is performed for two purposes. In the presence of oxygen in the cathode, hydrogen peroxide radicals are formed. With the oxidation of iron and its conversion to Fe^{2+}, Fenton reactions occur in the anodes. The radicals produced in response to the Fenton reactions increase the efficiency of the PNA and intermediate product degradation [14,15]. In addition to providing the oxygen required for redox reactions, aeration also supplies the force required to keep the reactor contents floating. This increases the contact between the charcoal and iron, increasing the number of microscopic galvanic cells and further enhancing the degradation efficiency [14]. With a further increase in aeration, no significant change was observed in the removal efficiency in the present study. On the other hand, further aeration increased costs and was not economical.

In micro-electrolysis systems, in the absence of oxygen, active species such as Fe^{2+} and [H], can participate in PNA degradation. However, the mineralization process is not complete, because the

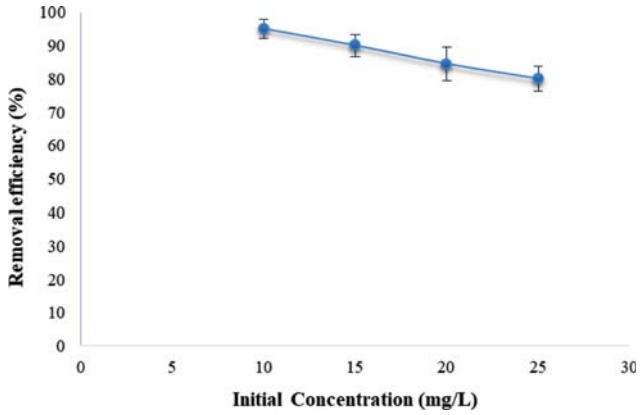

Fig. 5. Effect of primary PNA on removal efficiency under optimal conditions (Fe/charcoal: 2/1; time: 120 min; pH: 7; O_2: 10 L/min).

intermediate formed products are not easily degraded [15].

4. Effect of PNA Initial Concentration on Removal Efficiency

The results obtained from the effect of initial PNA concentration on the removal efficiency are shown in Fig. 5.

The maximum PNA removal occurred at 10 ppm. The PNA residual concentration in effluent of the reactor decreased to 0.5 mg/L after 120 min, which is lower than the TLV. An increase in the PNA concentration from 10 to 20 mg/L decreased the removal efficiency from 95 to 80%. The iron complexes produced in all solutions were the same, so the amount of flocs formed in the solutions was also the same. With a further increase in the PNA concentration, the flocs produced in the solution were not sufficient to absorb the intermediate compounds of the reaction and the PNA molecules. In addition, at low concentrations, more radicals were available for degrading the PNA molecules and reducing the intermediate compounds [28]. It is evident that, under the same operational conditions, a further elevation in the contaminant concentration could not produce a sufficient number of radicals in the electrochemical processes of the system to degrade the PNA molecules and the intermediate compounds. Thus, the extent of degradation was higher at lower concentrations [15].

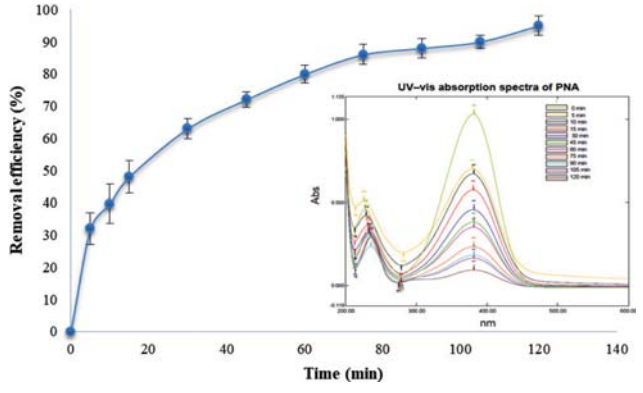

Fig. 6. Effect of contact time on PNA removal efficiency under optimal conditions (Fe/charcoal: 2/1; pH: 7; PNA: 10 mg/L; O_2: 10 L/min).

Wu et al. carried out micro-electrolysis of Cr (VI) using zero-valent iron coupled with active carbon [29]. With an elevation of the chromium concentration from 10 to 200 mg/L due to saturation of the active carbon surfaces and insufficiency of the degrading radicals, the removal efficiency decreased from 99% to 48%, which is in line with the results of the present study.

5. Effect of Contact Time on PNA Removal Efficiency

The results obtained from the effect of contact time of the reaction on PNA removal efficiency are shown in Fig. 6.

In the micro-electrolysis system, in the presence of oxygen, as the electrodes mixed together, microscopic galvanic cells formed quickly [14]. The reaction rate was high in the primary stages, such that in the first five minutes of the reaction, 32% of the PNA was removed. As the reaction progressed, degradation continued and the radicals produced in the micro-electrolysis system gradually degraded the PNA molecules, such that after a contact time of 120 min, the PNA removal efficiency reached 95%. The UV/vis spectrum in Fig. 6 demonstrates the trend of degradation of PNA molecules at a maximum wavelength of 381 nm for Fe/charcoal micro-electrolysis over time.

6. GC-MS Analysis of PNA Degradation Products and Proposed Process Pathway

Identification of the intermediate products in a degradation procedure provides valuable information to determine the degradation pathways of the analyte. A series of GC-MS analyses were performed to evaluate the possible mechanisms of PNA degradation by Fe/charcoal micro-electrolysis at 0, 5, 10, 15, 30, 60, 75, 90, 120, and 180 min to determine the structures of the intermediate compounds under the optimal conditions in the reactor. The structures of the main identified intermediates are shown in Table 1.

In comparison with the blank solution, a few peaks were observed in the chromatogram of the synthetic solution at retention times (t_R) of less than 27 min ($t_{R(PNA)}$). The structures of some of these chromatographic bands were determined by evaluating their respective mass spectra. Two peaks with t_R values of 16.2 and 19.2 min were identified as maleic acid (116 m/z) and benzoquinone (108 m/z), respectively, and were the major products of PNA decomposition. After evaluation and interpretation of the mass spectra of the products, the pathway shown in Fig. 7 was proposed for the PNA decomposition.

As shown in the proposed decomposition pathway (Fig. 7), following removal of the PNA functional groups and subsequent oxidation, the intermediate compounds decompose and are broken down into simpler molecules, which ultimately precipitate. In this

Table 1. Main intermediates of PNA degradation during Fe/charcoal micro-electrolysis as identified by GC-MS (Fe/charcoal: 2/1; pH: 7; PNA: 10 mg/L; O_2: 10 L/min)

Intermediate product	Chemical structure	t_R	m/z
Maleic acid	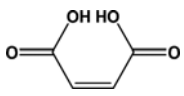	16.2	116
Benzoquinone	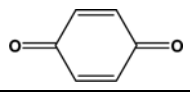	19.2	108

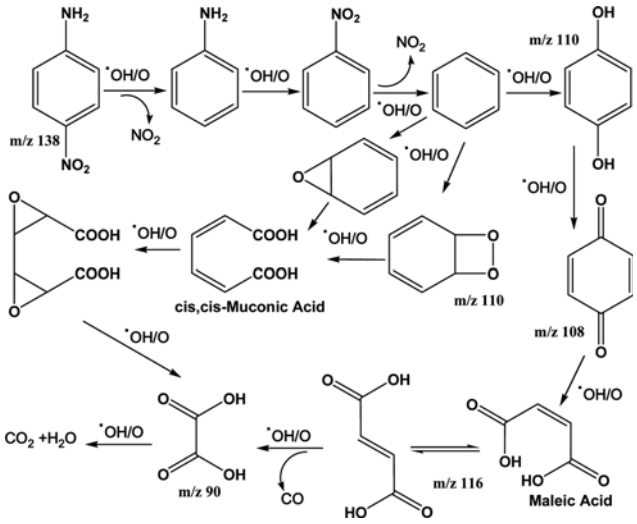

Fig. 7. Possible pathway for PNA degradation reaction.

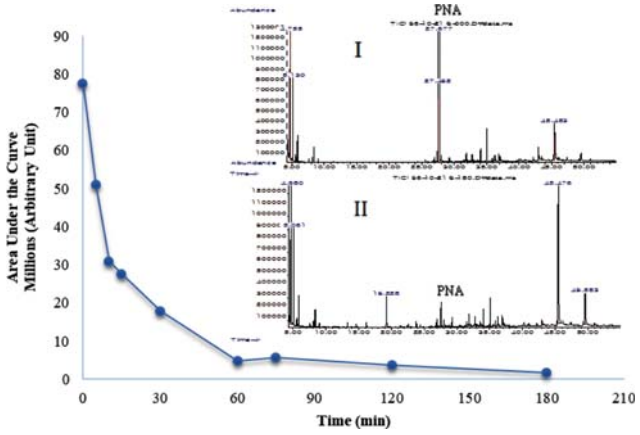

Fig. 8. Decrease in $AUC_{(PNA)}$ in reaction medium over time as identified by GC-MS (I: time zero; II: 180 min).

postulated oxidation pathway, with the loss of amine and nitro groups and the continuation of radical hydroxyl and oxygen attacks, the PNA converts to either hydroquinone (m/z 110) or benzene epoxide and benzene dioxetane (m/z 110) intermediates. Hydroquinone can be oxidized to benzoquinone, which in turn is oxidized and fragmented to maleic acid (a ring-opened product) under radical attack and oxidation. Furthermore, the carboxylic moieties of the maleic acid can lose neutral CO and are oxidized to oxalic acid. Next, oxalic acid is converted to inorganic compounds as reactions in the reactor are continued. In another postulated pathway, benzene epoxide and benzene dioxetane intermediates can arise *via* oxygen attack on the benzene ring, which can be subsequently broken to a ring-opened product as *cis, cis*-muconic acid. This intermediate similar to maleic acid can be fragmented more and broken down to oxalic acid following oxidation and the loss of CO.

A few studies have been carried out on the identification of the intermediates of PNA degradation [5,30,31]. The results of the present study differ from those of the previous ones, because the degradation method is quite different and results in different intermediate products on different decomposition pathways.

The decrease in the area under the curve (AUC) of the PNA peak over time in the reactor (0-180 min) was analyzed by GC-MS and is shown in Fig. 8.

The results of 3 h of monitoring of PNA degradation in the synthetic solution by GC-MS at 0, 5, 10, 15, 30, 60, 75, 90, 120, and 180 min show that the $AUC_{(PNA)}$ decreased significantly and the PNA level decreased up to 97% over time.

7. FTIR Analysis

FTIR spectroscopy of the sediment sludge was carried out at 500-4,000 cm^{-1}. The results are shown in Fig. 9.

In the FTIR spectrum of the sludge, symmetric and asymmetric stretching peaks of nitro (NO_2), which usually appear at about 1,350 and 1,550 cm^{-1}, were not observed. A lack of twin peaks for

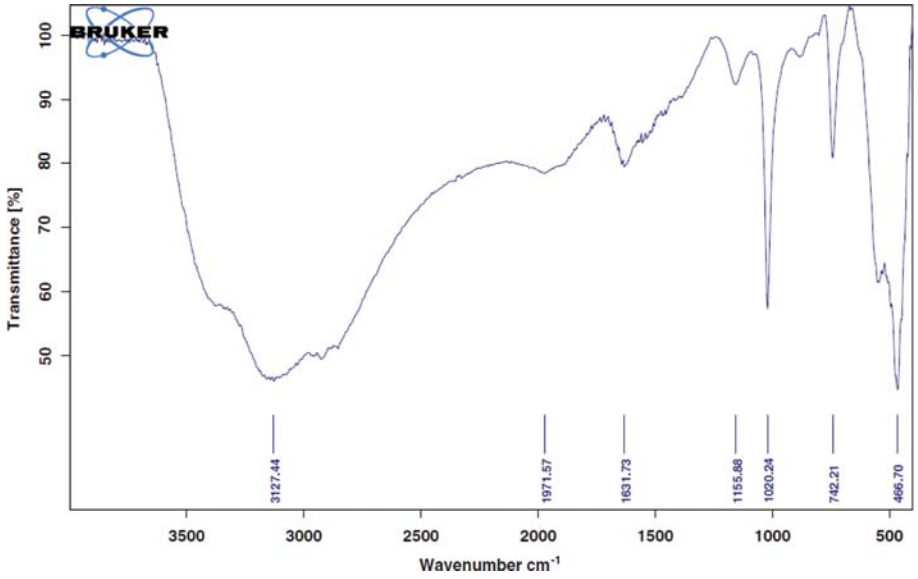

Fig. 9. FTIR spectrum of sludge from electrochemical processes of Fe/charcoal micro-electrolysis.

Table 2. The amount of iron ions measured in the solution by flame atomic absorption

Sample	Wavelength (nm)	Concentration of Fe ions (mg/L)
Blank sample (before the reaction)	248.3	Non detected
Reactor effluent (filtered)	248.3	Non detected

the NH_2 functional group can be indicative of the removal of these two moieties from the PNA molecule. A wide peak from about 2,400 to 3,600 cm^{-1} usually indicates O-H in the carboxylic acid moiety, which overlaps and covers the C-H stretching peak at about 3,000 cm^{-1}. The peak at wave number (1,631 cm^{-1}) is related to the C=O stretching bands which have shifted to a lower wave number due to probable conjugation. The strength of this peak is not usual and might be due to the low concentration of products. The peak observed at 1,020 cm^{-1} is representative of the C-O band and the carboxylic acid group. The peak at 742 cm^{-1} can be a determinant of an out-of-plate C-H bending vibration, and the peak at 466 cm^{-1} can be attributed to iron hydroxides [32]. Overall, the absence of NO_2 and NH_2 groups and the presence of the carboxylic in the reactor sludge is indicative of PNA oxidation followed by the breakdown of its aromatic ring on the path of degradation.

8. Secondary Pollution of Fe Ions

The atomic absorption spectrometry results of the investigation of secondary pollution of iron ions in the reaction solution of the reactor are shown in Table 2.

The results revealed that no iron ions were detectable by the atomic absorption spectrometer, which means that there could not be secondary pollution related to iron ions in the effluent of the reactor, and the iron ions were precipitated during the process as iron hydroxides in the sludge. Emerged peak at 466 cm^{-1} in FTIR spectrum of the sludge resulting from chemical reaction (Fig. 9) can be attributed to iron hydroxides [32], which confirms iron ions are deposited in sludge and are separated from the reactor's effluent.

9. Real Wastewater Sample

Table 3 presents the results of quality analysis of the real wastewater sample of the petrochemical industry and PNA removal efficiency under optimal conditions of the system.

The radicals produced in the micro-electrolysis system degraded the organic compounds non-selectively. In real wastewater, the presence of soluble organic compounds, suspended organic compounds, lipids, minerals and other soluble chemical compounds means that the radicals produced in the micro-electrolysis system were not sufficient. Furthermore, the iron hydroxide flocs were not sufficient for the adsorption and precipitation of these compounds. Therefore, the PNA removal efficiency declined from 95% in the synthetic solution to 89% in the real wastewater solution. Despite the presence of interfering compounds in the real wastewater sample, the PNA was largely removed. This large percentage of removal confirms the system efficiency.

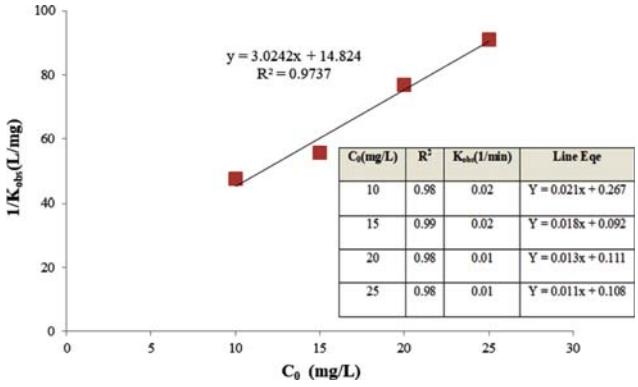

Fig. 10. *Pseudo*-first order kinetic and L-H model for different concentrations of PNA.

10. Degradation Kinetics

To investigate the PNA degradation kinetics in the micro-electrolysis system, a *pseudo*-first order kinetic model as well as the Langmuir-Hinshelwood (L-H) kinetic model were used. The linear form of the *pseudo*-first order kinetics is shown in Eq. (8) [19,33].

$$\mathrm{Ln}\,(C_t/C_0) = -K_{obs}\,t \tag{8}$$

The correlation coefficient was obtained by plotting Ln C/C_0 versus time at different PNA concentrations. The L-H model is shown in Eq. (9).

$$\frac{1}{K_{obs}} = \frac{1}{K_C K_{L\text{-}H}} + \frac{C_0}{K_C} \tag{9}$$

K_{obs} (min^{-1}) represents the first-order degradation rate constant, C_0 (mg L^{-1}) shows the initial PNA concentration, K_C (mg L^{-1} min^{-1}) denotes the superficial reaction rate constant and $K_{L\text{-}H}$ (L mg^{-1}) is associated with the adsorption equilibrium constant of the L-H model. To obtain the equilibrium constant of the L-H model and the superficial reaction rate, the $1/K_{obs}$ linear curve is plotted against the initial concentration [16].

The results of the *pseudo*-first order kinetic studies and L-H model are shown in Fig. 10.

In the investigation of the kinetic models, the correlation coefficient of the *pseudo*-first-order kinetics and L-H was 0.98 and 0.97, respectively. The high correlation coefficients suggest that PNA degradation kinetics can be explained by these models.

11. Stability of the System

Stability of the system was investigated in ten consecutive cycles under the optimum conditions (Fe/charcoal: 2/1; pH: 7; time: 120 min; PNA: 10 mg/L; O_2: 10 L/min). The results are shown in Fig. 11.

The PNA removal efficiency under the optimum conditions was

Table 3. Quality analysis of petrochemical wastewater sample and efficiency of PNA removal by Fe/charcoal micro-electrolysis under optimal conditions

Parameters	pH	COD (mg/L)	BOD_5 (mg/L)	TDS (mg/L)	TSS (mg/L)	SO_4^{-2} (mg/L)	Oil	PNA[a] (%)
Results	8.6	2500	850	2100	500	136	21	89

[a]Removal of efficiency by Fe/charcoal micro electrolyze reactor at optimum condition

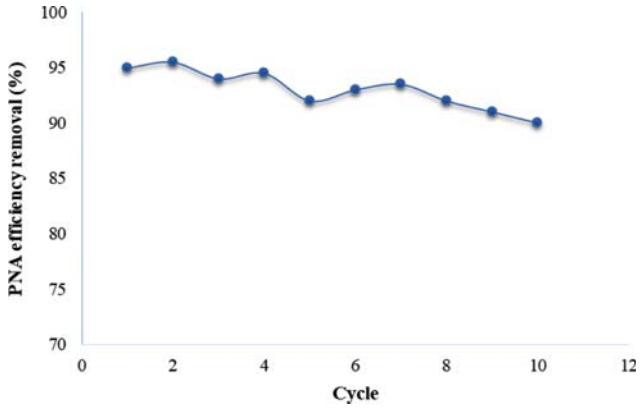

Fig. 11. PNA removal efficiency in ten consecutive cycles under optimum conditions (Fe/charcoal: 2/1; pH: 7; time: 120 min; PNA: 10 mg/L; O_2: 10 L/min).

95% in the first cycle and decreased to 90% in the tenths. Therefore, these systems do not require replacement of electrodes, and relevant reactions can occur as long as the iron has oxidation capability. In fixed-bed micro-electrolysis systems, due to the hardening, blockage and inactivation of Fe-C, the performance of the systems decreased sharply with the increasing operation time [15]. But in the Fe-charcoal reactor, due to electrode materials floating, the problems such as blocking and inactivation of iron-charcoal were resolved. In addition, the usage of cretacolor chunky charcoal resulted in the elevated stability of the system since the compressed carbon used in the reactor had slower corrosion and destruction resulting in high stability of the system.

12. Performance of the System Compared to Previous Studies

Some studies that have been carried out to remove PNA from aqueous solutions were compared with the present study. The results are shown in Table 4.

In many advanced oxidation processes, chemical oxidizing agents and other factors such as UV lamp are required to destroy organic compounds [26,33,34,37,38], which increases the cost in comparison with this micro-electrolysis system. In addition, many of these chemical agents are toxic and harmful to human health, and there are problems in the adsorption processes [35,36], such as non-destruction of pollutants and transfer of material from liquid phase to solid phase and adsorbent saturation.

In this study, iron chips were obtained from iron waste that had been discarded by metalsmithing workshops and cretacolor chunky charcoal was used as the cathode electrode. Compared to electrodes of electrolysis systems, these materials are much cheaper, and the process of organic compounds degradation occurs without the use of chemical oxidant and energy source. Totally, the system has a simple low-cost operation procedure with a very high efficiency.

CONCLUSION

This study demonstrates that PNA can be efficiently degraded in aqueous solution by Fe/charcoal micro-electrolysis system. Small iron and compressed charcoal pieces were used as electrodes, and redox reactions occurred following the contact between these materials. The destructive radicals produced by the electrochemical processes could decompose PNA efficiently. During the degradation process, PNA was converted to ring-opened intermediate acids, which finally could be mineralized in different pathways in a series of consecutive reactions. The highest degradation efficiency of PNA in petrochemical wastewater obtained 89% at pH: 7; contact time 120 min; aeration rate 10 L/min; Fe/charcoal ratio: 2/1; initial concentration of PNA: 10 mg/L. The kinetic of PNA degradation followed a *pseudo*-first order kinetic and the Langmuir-Hinshelwood model. Therefore, the Fe/charcoal semi-fluidized micro-electrolysis reactor, as a new method of advanced oxidation, has high efficiency in removing and degrading toxic and resistant compounds such as PNA from aqueous solutions and is recommended for this purpose.

ACKNOWLEDGEMENTS

This research was conducted at the Environmental Health Engineering Research Center and was sponsored by the Vice-Chancellor for Research and Technology of Kerman University of Medical Sciences. Appreciation is expressed here to the Vice-Chancellor and

Table 4. Comparison of this system with previous studies regarding the chemical used and optimum conditions

Chemical agents used in the reactor	Optimum conditions	Ref.
Waste Iron pieces, compressed charcoal	pH: 7; time: 120 min; PNA: 10 mg/L; O_2: 10 L/min, Fe/charcoal: 2/1	This research
H_2O_2, Ferrous sulfate ($FeSO_4{\cdot}7H_2O$)	$[PNA]_0$=0.181 Mm, $[Fe^{2+}]_0$=0.05 Mm, $[H_2O_2]_0$=10 Mm, pH=3.00, temperature=20±1 °C	[26]
Sodium persulfate ($Na_2S_2O_8$, 99%), Ferrous sulfate ($FeSO_4{\cdot}7H_2O$, 99%), Ferric chloride ($FeCl_3{\cdot}6H_2O$, 99%), Ammonia water ($NH_3{\cdot}H_2O$, 25-28%), Methanol (CH_3OH, 99%)	pH=7.0±0.2, T=25 °C, $[Na_2S_2O_8]_0$=8.0 mmol/L, $[Fe_3O_4]_0$=5.32 g/L $[PNA]_0$=0.2 mmol/L	[34]
Potassium dihydrogen phosphate, Ammonium chloride	V: 100 mL; C_0: 200 mg L^{-1}; pH: 7.6; CS-ACF dose: 0.30 gL^{-1}; T: 298 K; agitation rate: 150 rpm; contact time: 48 h	[35]
Zinc chloride, 4-methylbenzoic acid, Ethanol, *o*-dichlorobenzene, Nitrobenzene	Contact time: 250 min, pH: 4, 303 K	[36]

to all university staff who provided assistance to make this study possible.

REFERENCES

1. C. Nwokem, C. Gimba, G. Ndukwe and S. Abechi, *J. Adv. Sci. Res.*, **5**, 2 (2014).
2. C. Lai, B. Li, M. Chen, G. Zeng, D. Huang, L. Qin, X. Liu, M. Cheng, J. Wan, C. Du, F. Huang, S. Liu and H. Yi, *Int. J. Hydrogen Energy*, **43**, 3 (2018).
3. J. H. Sun, S. P. Sun, M. H. Fan, H. Q. Guo, Y. F Lee and R. X Sun, *J. Hazard. Mater.*, **153**, 1-2 (2008).
4. M. Malakootian, M. H. Ehrampoush, H. Mahdizadeh and A. Golpaygani, *J. Water Chem. Technol.*, **40**, 6 (2018).
5. S. Silambarasan and A. S. Vangnai, *J. Hazard. Mater.*, 302 (2016).
6. W. S. Chen and C. P. Huang, *Chemosphere.*, 125 (2015).
7. M. A. Oturan, *Environ. Sci. Pollut. Res.*, **21**, 14 (2014).
8. C. Lai, M. M. Wang, G. M. Zeng, Y. G. Liu, D. L. Huang, C. Zhang, R. Z. Wang, P. Xu, M. Cheng, C. Huang, H. P. Wu and L. Qin, *Appl. Surf. Sci.*, **390**, 30 (2016).
9. B. Li, C. Lai, G. Zeng, L. Qin, H. Yi, D. Huang, C. Zhou, X. Liu, M. Cheng, P. Xu, C. Zhang, F. Huang and S. Liu, *ACS Appl. Mater. Interfaces*, **10**, 22 (2018).
10. J. Kim, C. Yeom and Y. Kim, *Korean J. Chem. Eng.*, **33**, 6 (2016).
11. H. Lin, Y. Lin and L. Liu, *J. Taiwan Inst. Chem. Eng.*, 58 (2015).
12. M. Malakootian, H. Mahdizadeh, A. Nasiri, F. Mirzaienia, M. Hajhoseini and N. Amirmahani, *Desalination*, 438 (2018).
13. G. Hosseini, A. Maleki, H. Daraei, E. Faez and Y. Dadban Shahamat, *Arab. J. Sci. Eng.*, **40**, 11 (2015).
14. Z. Yang, Y. Ma, Y. Liu, Q. Li, Z. Zhou and Z. Ren, *Chem. Eng. J.*, 315 (2017).
15. H. Yanhe, L. Han, L. Meili, S. Yimin, L. Cunzhen and C. Jiaqing, *Sep. Purif. Technol.*, 170 (2016).
16. L. H. Liu, Y. Lin and Q. He, *Adv. Mater. Res.*, 955-959 (2014).
17. O. Yahiaoui, L. Aizel, H. Lounici, N. Drouiche, M. Goosen, A. Pauss and N. Mameri, *Desalination*, 270 (2011).
18. K. Baek, H. H. Lee, H. J. Shin and J. W. Yang, *Korean J. Chem. Eng.*, **17**, 2 (2000).
19. H. Zhou, P. Lv, Y. Shen, J. Wang and J. Fan, *Water Res.*, **47**, 10 (2013).
20. B. Lai, Y. Zhou, P. Yang, J. Yang and J. Wang, *Chemosphere.*, **90**, 4 (2013).
21. S. Deng, D. Li, X. Yang, W. Xing, J. Li and Q. Zhang, *Chemosphere.*, 168 (2017).
22. J. Shi, B. Zhang, S. Liang, J. Li and Z. Wang, *Environ. Sci. Pollut. Res.*, **25**, 9 (2018).
23. M. A. Oturan, J. Peiroten, P. Chartrin and A. J. Acher, *Environ. Sci. Technol.*, **34**, 16 (2000).
24. W. Huang and R. Liu, *Adv. Mater. Res.*, 233-235 (2011).
25. APHA, AWWA, WEF. Standard Methods for the Examination of Water and Wastewater, Ed. 20. USA (1998).
26. J. H. Sun, S. P. Sun, M. H. Fan, H. Q. Guo, L. P. Qiao and R. X. Sun, *J. Hazard. Mater.*, **148**, 1-2 (2007).
27. A. Khataee and M. Zarei, *Desalination*, **278**, 1-3 (2011).
28. M. Malakootian, M. Pourshaban-Mazandarani, H. Hossaini and M. H. Ehrampoush, *Process Saf. Environ. Prot.*, **104**, Part A (2016).
29. L. Wu, L. Liao, G. Lv, F. Qin, Y. He and X. Wang, *J. Hazard. Mater.*, **254-255**, 15 (2013).
30. O. A. Zelekew and D. H. Kuo, *Appl. Surf. Sci.*, **393**, 30 (2017).
31. S. Gautam, S. P. Kamble, S. B. Sawant and V. G. Pangarkar, *Chem. Eng. J.*, **110**, 1-3 (2005).
32. M. Mecozzi, E. Sturchio, P. Boccia, M. Zanellato, C. Meconi and F. Peleggi, *Environ. Sci. Pollut. Res.*, **24**, 6 (2017).
33. X. Zhou, C. Lai, D. Huang, G. Zeng, L. Chen, L. Qin, P. Xu, M. Cheng, C. Huang, C. Zhang and C. Zhou, *J. Hazard. Mater.*, 346 (2018).
34. Y. S. Zhao, C. Sun, J. Q. Sun and R. Zhou, *Sep. Purif. Technol.*, 142 (2015).
35. K. Li, Z. Zheng, J. Feng, J. Zhang, X. Luo, G. Zhao and X. Huang, *J. Hazard. Mater.*, **166**, 2-3 (2009).
36. K. Zheng, B. Pan, Q. Zhang, W. Zhang, B. Pan, Y. Han, Q. Zhang, D. Wei, Z. Xu and Q. Zhang, *Sep. Purif. Technol.*, **57**, 2 (2007).
37. B. Kamarehie, J. Mohamadian, S. A. Mousavi, G. Asgari and Y. Dadban Shahamat, *Desalination Water Treat.*, 80 (2017).
38. A. Benito, A. Penadés, J. L. Lliberia and R. Gonzalez-Olmos, *Chemosphere.,* 166 (2017).